Old Dominion University

ODU Digital Commons

1988

Raman Scattering Characterization of the Microscopic Structure of Semi-Insulating Polycrystalline Si Thin Films

D.J. Olego

H. Baumgart
Old Dominion University, hbaumgar@odu.edu

Raman scattering characterization of the microscopic structure of semi-insulating polycrystalline Si thin films

D. J. Olego and H. Baumgart

Philips Laboratories, North American Philips Corporation, Briarcliff Manor, New York 10510

Raman scattering experiments were carried out to study the microscopic structure of semi-insulating polycrystalline Si (SIPOS) thin films prepared by low-pressure chemical vapor deposition. The samples contain 18, 25, and 30 at. % of oxygen and after growth they were annealed at 900 and 1000 °C for 30 min. The Raman spectra show in the vibrational region of the optical frequencies of Si two bands, which arise from scattering in crystalline grains and disordered forms of Si. The behavior of these bands as a function of oxygen content and annealing temperatures was established in detail. The crystallinelike band peaks below the transverse optical frequency of Si at zone center and is broadened with respect to the Raman line of a Si wafer. From the broadenings, estimates of grain sizes are obtained. The band due to the disordered form of Si appears at frequencies above those of an extended network of amorphous Si. A model for the SIPOS microscopic structure is proposed in which the disordered Si corresponds to the surface layers of the crystalline grains. The latter are embedded in an amorphous SiO_2 matrix. Quantitative estimates of the contributions of the ordered and disordered phases of Si to the SIPOS structure are attempted. The Raman results provide additional experimental evidence that the crystallization temperature of Si increases under the presence of oxygen.

I. INTRODUCTION

Semi-insulating polycrystalline silicon (SIPOS) thin films, also known as silicon-rich silicon dioxide or oxide (SRO), have attracted considerable attention for applications in various types of Si devices. Hence, the characterization of the intrinsic properties of this system has been actively pursued in recent years.[1-10] The present work deals with the nature of the microscopic structure of SIPOS thin films, which from a chemical standpoint can be regarded as a mixture of silicon (Si) and oxygen (O) with an effective composition given by SiO_x. In general, the amount of oxygen x ranges between 10 and 40 at. %. However, from a physical point of view the description of the microscopic nature of SIPOS is more complex. The difficulties arise in part due to the properties of the Si-O phase diagram and also because of the thermal treatments required in the applications SIPOS are intended for. Thin films of SIPOS are commonly deposited at substrate temperatures above 550 °C and post-deposition annealings at temperatures in excess of 900 °C are routinely performed. At these temperatures x exceeds the solubility limits of O in Si and the microscopic structure of SIPOS becomes a multicomponent mixture. In annealed specimens, one of the components has been identified to be SiO_2 in several studies.[1-3] The other components are related to various forms of Si and crystalline and amorphous Si have been detected.[1,2,4,7-9] However, the characterization of the Si-rich components of SIPOS is far from complete. The interplay between crystalline and amorphous forms of Si and their relationships with x and thermal treatments are not well established, even though they are relevant for the interpretation of transport and electro-optical characteristics of SIPOS devices.

We report here on a Raman scattering characterization of the nature of the microscopic structure of SIPOS thin films with emphasis on the analysis of the Si-rich phase. Raman scattering is a suitable technique to detect different forms of Si and has been extensively applied in the characterization of polycrystalline and amorphous thin films of Si as well as SiO_x.[2,4,11,12] In our experiment, contributions to the Raman intensities are measured that arise from scattering in crystalline and disordered Si. These contributions are studied as a function of x and annealing temperatures, and are compared to the case of polycrystalline Si samples without O. Based on the results we propose a model for the microscopic structure of SIPOS, in which the disordered Si component constitutes the surface layer of crystalline grains of Si. In addition, we confirm earlier reports that the crystallization temperature of Si increases with the presence of O.[4,9]

The paper is organized in the following way: the next section describes the experimental part of sample preparation and optical measurements and Sec. III relates to the Raman results. We discuss these results and propose a model based on them for the microscopic structure in Sec. IV. Finally, the conclusions are presented in Sec. V.

II. EXPERIMENT

The SIPOS thin films (typical thicknesses 0.3–0.5 μm) were deposited on (100) Si substrates from the decomposition of SiH_4 and N_2O in a low-pressure chemical vapor deposition reactor. The substrate temperature during growth was 650 °C and the background reactor pressure ranged between 0.2 and 0.5 Torr. The O content x in the films was changed by adjusting the ratio of SiH_4 to N_2O. Ratios between 5–10 were used to obtain samples with 18, 25, and 30 at. % of O. These values of x were confirmed by energy dispersive analy-

sis of x rays (EDAX), infrared transmission, and gravimetric and differential thickness analysis. After deposition the samples were thermally annealed in an inert atmosphere at temperatures $T_A \approx 900$ and 1000 °C for 30 min. No degradation of the film morphology was observed after the annealings. Infrared transmission performed on the samples revealed for the as-deposited films stretching Si-O vibrations with frequencies in the range 1020–1050 cm^{-1} scaling with the composition SiO_x.[13] For the annealed samples, only SiO_2 stretching vibrations at 1085 cm^{-1} were observed for all values of x, which indicates the presence of the SiO_2 phase in the network of the films. No other foreign elements such as N or H were detected in the films. Characterization of the samples with Auger and x-ray photoelectron spectroscopies yielded that N is not present within the detection limits of the techniques which were estimated to be better than 0.5 at. %. In addition, no absorption lines at around 840 cm^{-1} due to Si-N vibrations and at around 630, 880, and 2000 cm^{-1} due to Si-H modes were observed in the infrared transmission spectra of the SIPOS films.

The Raman scattering measurements were carried out at room temperature with incoming light at 5145 Å in the backscattering configuration. The scattered light was dispersed by a double monochromator with a resolution better than 0.4 cm^{-1} and detected with photon counting electronics. The polarization of the incoming photons was in the plane of incidence and the scattered polarization was not analyzed.

III. RESULTS

Typical Raman spectra for SIPOS samples with different values of x, which have been annealed at $T_A \approx 900$ °C, are displayed in Fig. 1. The curves are plotted against the Stokes shifts in the spectral region of the optical frequencies of Si. For comparison purposes, the first-order Raman spectra of a crystalline Si wafer and that of an as-deposited SIPOS film are included. The spectrum of the crystalline wafer shows the narrow line at ≈ 520 cm^{-1} due to scattering by the long wavelength transverse optical phonons. The line shapes of the spectra corresponding to the as-deposited SIPOS are independent of the values of x. They display two broader bands characteristic of amorphous Si with the stronger one peaking at around 480 cm^{-1}. For the case of the annealed samples, the Raman spectra in the range 480–520 cm^{-1} consist of two bands with Stokes shifts in between the frequencies of the crystalline and amorphous examples. These bands have been labeled I^d and I^c in Fig. 1 for reasons which will become apparent in the subsequent discussions. We observe that the I^c peaks are shifted to lower frequencies and are somewhat broadened with respect to the crystalline Raman line. The shifts and broadenings increase with x for a given T_A. Typical measured shifts for $T_A \approx 900$ °C and $x = 18, 25, 30$ at. % of O are -1, -3.2, and -7.6 cm^{-1}, respectively. The corresponding broadenings are 1.3, 12, and 15 cm^{-1}, respectively. On the other hand, the structures I^d are shifted to higher frequencies when compared with the prominent feature of the amorphous samples at 480 cm^{-1}. These shifts to higher frequencies are larger the smaller the x value. In the spectra of the annealed specimens, we do not detect the typi-
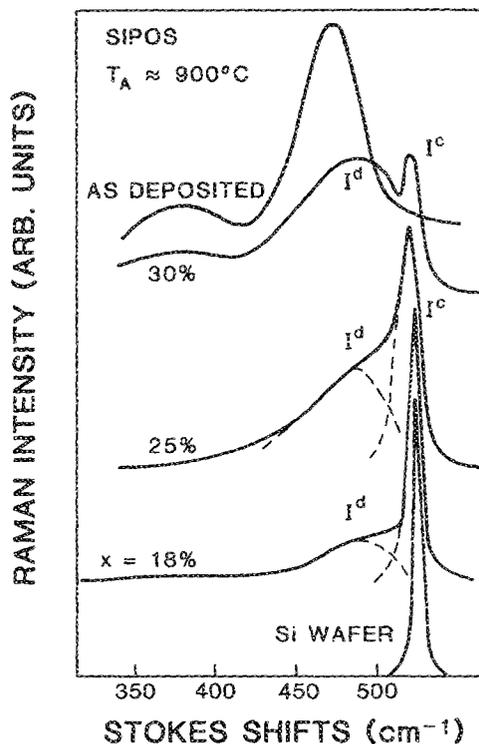
FIG. 1. Raman spectra of SIPOS thin films as a function of O content x for a given annealing temperature T_A. The spectra of a single-crystal Si wafer and of an as-deposited SIPOS thin film are included for comparison. The structures labeled I^c and I^d in the annealed samples arise from scattering in ordered and disordered forms of Si present in the SIPOS network, respectively. The dashed lines represent the deconvolution of the intensities of I^c and I^d. The crystallinelike bands I^c peak below the Raman line of the wafer and are wider than it. Note that the I^d bands have larger Raman shifts than the characteristic peak of amorphous Si at ≈ 480 cm^{-1} seen in the spectrum of the as-deposited samples.

cal Raman signal of SiO_2 at around 450 cm^{-1}. We were able to measure this signal only with an all SiO_2 film several micrometers thick. However, under similar conditions as those used to collect the data of all the SIPOS, the strength of the SiO_2 Raman signal was at least two orders of magnitude weaker than in the spectra displayed in Fig. 1. Therefore, the lack of the SiO_2 signature in the SIPOS data is attributed to the inherent weakness of this signal and the small scattering volume available in the SIPOS films which are much thinner than the SiO_2 film used for testing.

The behavior of the Raman spectra for a given x and changing T_A is represented in Fig. 2. When the annealing temperature is increased, both I^c and I^d shift slightly to higher frequencies. In addition, the relative intensity of I^d diminishes and I^c becomes sharper. The ratios of integrated intensities under the deconvoluted structures of Figs. 1 and 2 assuming symmetrical line shapes are tabulated in Table I. The ratios I^d/I^c decrease with increasing T_A for fixed x, and conversely increase with x for a constant T_A. It is expected that for T_A larger than those investigated here the contribution of I^d will become negligible. Similar spectra to those in Figs. 1 and 2 can be found in the literature.[2,4] However, the behaviors of I^c and I^d (intensities and frequencies) have not been studied with the level of detail presented here. It is this kind of analysis that provides the framework for the
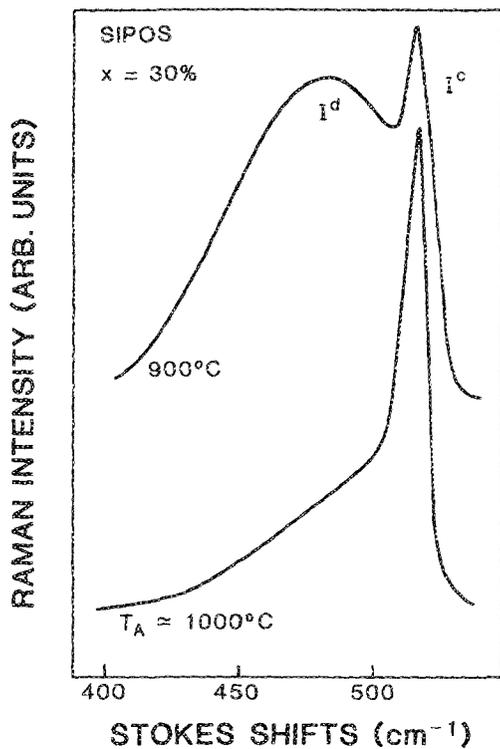
FIG. 2. Evolution of the Raman spectra of SIPOS for a given value of x and changing annealing temperature T_A. With increasing T_A both Raman bands I^c and I^d shift slightly to higher frequencies. The relative intensity I^d/I^c decreases and I^c becomes narrower.
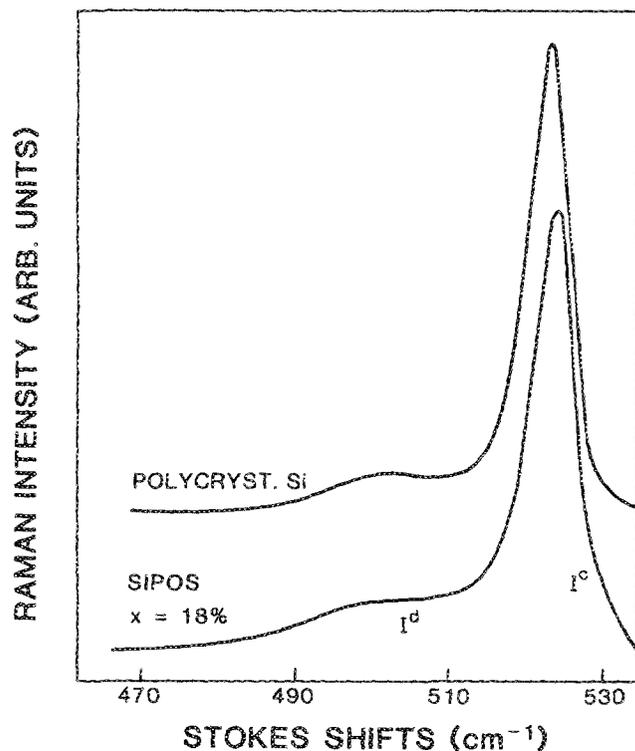
FIG. 3. Comparison of the Raman spectra of an annealed SIPOS sample and of a thin film of polycrystalline Si. There is a strong resemblance between both line shapes which reinforces the interpretation of the I^c and I^d Raman lines in the SIPOS case as being related to the Si-rich phase.

characterization of the microscopic network discussed in the next section.

The spectra of the annealed SIPOS specimens in the spectral range under consideration are strikingly similar to those observed in some instances for polycrystalline Si samples without any O. We illustrate this point in Fig. 3 by comparing the spectra of a SIPOS film with that of a polycrystalline Si thin film grown in our laboratory, also by low-pressure chemical vapor deposition. Two bands are measured for the polycrystalline sample, which resemble the I^d and I^c structures in the SIPOS spectra. It is important to mention that the broader I^d-like band appears also well above 480 cm^{-1} in the all Si material. The appearance of such a band was reported earlier in polycrystalline Si prepared by plasma-assisted deposition.[11] The results in Fig. 3 prove that the vibrational states responsible for it do not depend exclusively on growth methods. Pertinent to the present work, the comparison in Fig. 3 establishes that I^c and I^d are related to scattering by modes of the Si-rich phase in the SIPOS microscopic network.

IV. DISCUSSIONS

The Raman line shapes shown in Figs. 1–3 provide an insight into the microscopic structure of the annealed SIPOS. The simultaneous appearance of I^c and I^d is taken as an indication of the presence of crystalline (I^c) and disordered (I^d) Si in the network of the SIPOS thin films.[2,4,11,12] We recall that the other phase is SiO_2 as confirmed by the infrared transmission properties of our annealed samples and by characterization experiments performed by others in

comparable samples.[1-4] Furthermore, the behavior of I^c and I^d with T_A and x allows some quantification of the properties of the Si components. The shifts to lower frequencies and broadenings of I^c with respect to the Raman line of a crystalline Si wafer are indicative of wave vector nonconservation in the scattering process, which occurs when the ordered Si forms grains. The average diameters d of the grains can be inferred from the I^c broadenings according to the prescription given for example by Eq. 2.117 in Ref. 12. The so-determined values of d are tabulated in Table I. With increasing x smaller grains are obtained for a constant T_A. On the other hand, the grains become larger with increasing T_A in a fashion similar to the trends found in polycrystalline Si.[11,14] Grains of crystalline Si have been observed in transmission electron microscopy experiments done in SIPOS.[1,7,8] There is a good overall agreement between grain sizes established with electron microscopy and the values in Table I.

The I^d structures are interpreted as arising from scattering by vibrational modes of disordered Si. However, it has to

TABLE I. Relative intensities of the I^d and I^c Raman bands shown in Figs. 1 and 2 and estimated grain sizes from the broadenings of I^c.

$x(\%)$	I^d/I^c		$d(\text{Å})$	
	900 °C	1000 °C	900 °C	1000 °C
18	0.75	0.4	80	100
25	1.4	0.6	26	50
30	2.5	0.9	20	30

be kept in mind that the I^d frequency shifts are above those well documented for the main peak of amorphous Si at $\approx$480 cm^{-1}. In addition, an interplay exists between the intensities and shifts of I^d and I^c, which suggests an intimate relationship between the ordered and disordered components of Si. Therefore, we conclude that the state of the disordered phase of Si is different from that of an extended amorphous Si network. Similar to the analysis done for polycrystalline Si, the I^d bands are interpreted as the vibrational modes of surface layers of disordered Si around the Si grains.[11] Supportive evidence for this interpretation is given by theoretical calculations which predict values between 480 and 520 cm^{-1} for shearing modes of Si in disordered surface layers,[15,16] and the empirical observation that the intensity ratios I^d/I^c correlate with the ratios of the surface to volume number of Si atoms.[11] With increasing d (because of higher T_A or smaller x) it is easy to calculate by approximating the grains to be spheres of diameter d that the surface to volume ratio of Si atoms diminishes. The same trend takes place for the ratio I^d/I^c according to the values in Table I.

The Raman data cannot distinguish if the Si grains in the SIPOS are disconnected from one another or interconnected through the disordered surface layers acting as grain boundaries, as expected in the case of polycrystalline Si. But transport properties measurements performed in a set of samples with the same specifications and growth conditions as the ones used in this experiment have established that the conduction process takes place by the tunneling of carriers between the Si grains through barriers of SiO_2.[5] In other words, the Si grains are electrically insulated from each other. With this additional information in mind, we model the microscopic structure of the annealed SIPOS as illustrated in Fig. 4. The crystallites of Si, which are surrounded by the disordered Si shells, are embedded in the amorphous SiO_2

matrix. This model for the microscopic structure, drawn with the consideration of low-field transport properties, supports the interpretation of electroluminescence studies done in SIPOS,[6] and is consistent with results of structural and electro-optical characterizations.[2,4,7] It is in disagreement with the "mosaic structure" model, in which an underlying amorphous Si matrix is assumed.[1] The latter structure has been recently invoked to explain high-field electrical conduction experiments.[10] However, it can be argued that given the multiphase microscopic nature of SIPOS high-field effects may not have the ability to distinguish between the two models.

The atomic percent contributions of Si atoms to the ordered Si component (N^c) and disordered one (N^d) can be quantified if one assumes that the intensity ratios I^d/I^c can be normalized by the ratios of the absolute Raman cross sections for amorphous and crystalline Si. This ratio is $\approx$0.15 for modes in the frequency range 400–500 cm^{-1} and exciting light at 5145 Å.[17] Multiplying I^d/I^c by 0.15 gives a determination of the ratio N^d/N^c, which together with the boundary condition $N^c + N^d + N^{Si-O} + N^O = 100\%$ allows to obtain the values quoted in Table II. The O composition x is represented by N^O and N^{Si-O} is the atomic percent of Si atoms bonded to O and forming the SiO_2 phase. These two quantities are fixed by the growth in the case of the annealed samples because almost all the O atoms are present in the SiO_2 phase. The numbers in Table II critically depend on the validity of the normalization by the absolute Raman scattering cross sections and the value of the normalization factor. Both aspects have to be secured by further experimental work. Notwithstanding these arguments, the values in Table II mirror very clearly the trends discussed throughout namely that, for a given T_A, N^d increases with x at the expenses of N^c because the crystalline grains become smaller.

Disordered forms of Si are present in SIPOS samples which have been heated well above the crystallization temperature T_c of Si. This experimental observations given by the spectra in Figs. 1 and 2 establish that the T_c of Si increases with the presence of O. Indeed the ratios I^d/I^c of Table I indicate that T_c is a strong function of x. The increase in T_c of Si in SIPOS was realized before,[4,9] and is fully consistent with the same effect seen in other amorphous systems.[18]

V. CONCLUSIONS

We have presented a Raman scattering characterization of SIPOS thin films in which we studied in detail the proper-

FIG. 4. Proposed model for the microscopic structure of annealed SIPOS thin films. Grains of crystalline Si with average cross section d are surrounded by a surface layer of disordered Si in an underlying matrix of amorphous SiO_2. The size of the grains and the relative contribution of the disordered to the ordered component depend on x and T_A according to the values summarized in Tables I and II.

TABLE II. Atomic percent contributions of O and Si atoms for a sample annealed at 900 °C to the SiO_2 phase ($N^O = x$ and N^{Si-O}, respectively) and to the ordered and disordered Si component (N^c and N^d, respectively).

N^O	N^{Si-O}	N^c	N^d
18	9	66	7
25	12.5	52	10
30	15	41	14

ties of the Si-rich phase of the microscopic network. This phase consists of crystalline grains and disordered Si, whose relative contributions were found to depend strongly on O content and thermal treatments. We interpreted the nature of the disordered form of Si as being different from that of an extended structure of amorphous Si. It was concluded that disordered Si in the SIPOS corresponds to the surface layers of the Si grains. A model for the SIPOS microscopic structure was elaborated based on the Raman results and published low-field transport characteristics. The atomic percent contributions of Si atoms to the crystalline and disordered forms were quantified by assuming a normalization of the measured Raman intensities. The SIPOS thin films constitute an interesting model system in which to investigate the properties of the Si-O phase diagram. For example, we have shown that the crystallization temperature of Si is a strong function of the O content.

ACKNOWLEDGMENTS

[1] M. Hamasaki, T. Adachi, S. Wakayama, and M. Kikuchi, J. Appl. Phys. **49**, 3987 (1978).

[2] A. M. Goodman, G. Harbeke, and E. F. Steigmeier, in *Physics of Semiconductors*, edited by D. L. H. Wilson (Institute of Physics, London, 1979), p. 805.

[3] J. H. Thomas III and A. M. Goodman, J. Electrochem. Soc. **126**, 1766 (1979).

[4] A. Harstein, J. C. Tsang, D. J. DiMaria, and D. W. Dong, Appl. Phys. Lett. **36**, 836 (1980).

[5] J. Ni and E. Arnold, Appl. Phys. Lett. **39**, 559 (1981).

[6] D. J. DiMaria, J. R. Kirtley, E. J. Pakulis, D. W. Dong, T. S. Kuan, F. L. Pesavento, T. N. Theis, J. A. Cutro, and S. D. Brorson, J. Appl. Phys. **56**, 401 (1984); and references therein.

[7] J. Wong, D. A. Jefferson, T. G. Sparrow, J. M. Thomas, R. H. Milne, A. Howie, and E. F. Koch, Appl. Phys. Lett. **48**, 65 (1986).

[8] H. Baumgart, E. Arnold, J. Petruzzello, T. F. McGee, and M. H. Frommer in *Comparison of Thin Film Transistors and SOI Technologies*, edited by H. W. Lam and M. J. Thompson, Mater. Res. Soc. Symp. Proc. **33**, (Elsevier Science, New York, 1984), p. 87.

[9] L. A. Nesbit, Appl. Phys. Lett. **46**, 38 (1985).

[10] R. B. Comizzoli and R. L. Opila, J. Appl. Phys. **61**, 261 (1987).

[11] Z. Iqbal and S. Veprek, J. Phys. C **15**, 377 (1982).

[12] See discussions in the review article by M. Cardona, in *Light Scattering in Solids II*, edited by M. Cardona and G. Güntherodt (Springer, Heidelberg, 1982), p. 19 and references therein.

[13] L. Schumann, A. Lehmann, H. Sobotta, V. Riede, U. Teschner, and K. Hübner, Phys. Status Solidi B **110**, K69 (1982).

[14] G. Harbeke, L. Krausbauer, E. F. Steigmeier, A. E. Widmer, H. F. Kappert, and G. Neugebauer, J. Electrochem. Soc. **131**, 675 (1984).

[15] W. Pollard and G. Lucovsky, J. Phys. (Colloq.) C4 **42**, 353 (1981).

[16] G. Kanellis, J. F. Morhange, and M. Balkanski, Phys. Rev. B **21**, 1543 (1980).

[17] D. Bermejo and M. Cardona, J. Non-Cryst. Solids **32**, 405 (1979).

[18] D. J. Olego, R. Schachter, and J. Baumann, Solid State Commun. **53**, 907 (1985).